LWT - Food Science and Technology 142 (2021) 111014

Contents lists available at ScienceDirect

LWT

journal homepage: www.elsevier.com/locate/lwt

Rheological characterisation of full-fat and reduced-fat aerated icings

Bárbara E. Meza [a], Rubens R. Fernandes [b], Susana E. Zorrilla [a], D. Ian Wilson [b], Juan Manuel Peralta [a,*]

[a] Instituto de Desarrollo Tecnológico para la Industria Química (INTEC), Universidad Nacional del Litoral (UNL) – Consejo Nacional de Investigaciones Científicas y Técnicas (CONICET), Güemes 3450, S3000GLN, Santa Fe, Argentina
[b] Department of Chemical Engineering and Biotechnology, University of Cambridge. Philippa Fawcett Drive, Cambridge, CB3 0AS, United Kingdom

ARTICLE INFO

Keywords:
Buttercream
Creep
Recovery
Fat replacement
Air volume fraction

ABSTRACT

Aerated icings are a sweet, fat-rich, and uncooked type of glaze material made by whipping sugar and fat together to form a bubbly fluid. The rheological behaviour of full-fat and reduced-fat aerated icings was characterised using rotational rheometry techniques. Control full-fat formulations were prepared using commercial icing sugar and unsalted butter (a viscoplastic fat-based continuous phase) in a 2:1 ratio. Reduced-fat samples were prepared by replacing 25% and 50% of butter by mass by a 50% w/w of native corn starch suspension (a potential carbohydrate-derived fat replacer). Icings with different air volume fractions were prepared by mixing in a planetary mixer for 3 min or 6 min (air volume fractions ≤ 0.17). The size distribution of sugar crystals and air bubbles were similar, with modal values near 10 μm. The experimental data from flow curves and creep tests were described well by the Bingham and Burgers models, respectively. Flow behaviour and static yield stress values were affected by the mixing time and the butter replacement, whereas the viscoelastic behaviour was only influenced by the latter. The information obtained in this study can be used to assess whether these reduced-fat products are suitable for the flow and coating stages of manufacturing.

1. Introduction

Aerated icing (frosting or buttercream) is a sweet, fat-rich, and uncooked type of glaze made by whipping powdered or table sugar and fat (butter and/or vegetable oil shortening) together to form a bubbly fluid (Gómez, 2008; McNeill, 2014). This confectionery material is used to coat baked goods and desserts for protective, flavouring, and decorative purposes.

In aerated foods such as icings, the whipping process provides energy to incorporate and entrap small air bubbles in the continuous phase (Campbell & Mougeot, 1999; Zúñiga & Aguilera, 2008). The presence of stable dispersed bubbles, where the timescale for coalescence and separation is long compared with the process timescale, gives rise to elasticity. In addition to sweetening, sugar crystals provide bulk and structure, being nuclei for aeration when fat is creamed (Campbell & Mougeot, 1999; Gómez, 2008). Unsalted butter is traditionally used as the continuous phase. However, butter is an animal-origin fat with highly saturated acids and cholesterol, which detract from a health and nutrition perspective (Rønholt, Mortensen, & Knudsen, 2013).

Reducing the butter content of icings is desired for reduced-fat food products (Meza, Peralta, & Zorrilla, 2016). Some aerated icing recipes include non-fat milk solids or powdered egg white to reduce the fat content and obtain a creamy texture without decreasing its stability (Glass, Murphy, & Santori, 1992; Morehouse & Lewis, 1985). The use of carbohydrate-based fat replacers is one strategy; it has been suggested for some time that starches could replace the lipids in foods as well as enhancing their stability, creaminess, and moisture retention (Lucca & Tepper, 1994). Native and modified starches have been used as fat replacers in low-fat stirred yogurts and bakery products (Lobato-Calleros, Ramírez-Santiago, Vernon-Carter, & Alvarez-Ramirez, 2014; Serinyel & Öztürk, 2016). Native starches from several sources can be consumed even without further treatment because they have partial digestibility (Singh, Dartois, & Kaur, 2010).

Replacing a component in a traditional recipe can affect its processing behaviour as well as the qualities of the final product. It is important to retain rheological characteristics of aerated icings so that they can be pumped, dispensed through nozzles and spread over baked foods. They must also retain sufficient residual structure to maintain a layer thickness (avoiding thinning) and shape (avoiding levelling) after application (Gómez, 2008). The latter characteristics can be achieved by

* Corresponding author.
E-mail address: jmperalta@intec.unl.edu.ar (J.M. Peralta).

https://doi.org/10.1016/j.lwt.2021.111014
Received 21 October 2020; Received in revised form 25 January 2021; Accepted 28 January 2021
Available online 6 February 2021

Table 1
Recipes (mass and volume fractions) used to prepare aerated icings for food coating.

Code	Mass fraction (Estimated volume fraction[b]) [% w/w] ([-])		
	Icing sugar	Butter	CSS[a]
Control	66.6 (0.54)	33.4 (0.46)	0.0 (0.00)
25% BR	66.6 (0.56)	25.0 (0.35)	8.4 (0.09)
50% BR	66.6 (0.57)	16.7 (0.24)	16.7 (0.19)

[a] CSS = 50% (w/w) native corn starch suspension.
[b] Volume fractions estimated with Eq. (1) using densities obtained from literature: starch, 1500 kg m^{-3}; butter 950 kg m^{-3}; and sugar, 1588 kg m^{-3} (Rahman, 2009).

using a viscoplastic fluid as the continuous phase.

Knowledge of the rheological behaviour of a film-forming material is required for selecting deposition techniques and optimising coating process design (Eley, 2005; Shay, 1995). Viscoelastic models have been used to evaluate material structure before and after coating, as well as film levelling capacity (Eley, 2005). Bubbly fluids pose challenges as their rheology is determined both by the behaviour of the continuous phase and by the bubble volume fraction (Torres, Gadala-Maria, & Wilson, 2013; Torres, Hallmark, & Wilson, 2015a,b). A secondary factor is creaming, where the buoyancy of bubbles drives phase separation over longer time scales. This is avoided with icings using shear-thinning or viscoplastic continuous phases. Butter is considered a viscoplastic material (Right, Canlon, Hartel, & Marangoni, 2001; Vélez-Ruiz, Barbosa Cánovas, & Peleg, 1997) but exhibits viscoelastic behaviour at low deformation rates over the melting range of milk fat. Native starch suspensions have been extensively studied and identified with shear-thinning or shear-thickening properties, depending on concentration and the shear rate (Chesterton, Pereira de Abreu, Moggridge, Sadd, & Wilson, 2013; Wang, Wang, Li, Zhou, & Özkan, 2011).

The objective of this work was to characterise the rheological behaviour of a set of aerated icings used for food coating applications. Formulations were prepared using a viscoplastic fat-based continuous phase (butter) with different contents of a native starch suspension (potential carbohydrate-derived fat replacers with shear-thickening or shear-thinning properties, depending on concentration used and shear rate applied), to simulate an aerated icing with reduced lipid content. To the knowledge of the authors, the effect of replacing part of a viscoplastic continuous phase with a shear-thickening (or shear-thinning) component in aerated icings has not been studied systematically to date. Different rheometric techniques were employed to characterise these coatings, probing different stages in processing. The information generated can be used to evaluate whether new reduced-fat coating products are feasible, saving time and minimising trial-and-error testing.

2. Materials and methods

2.1. Aerated icing preparation

Commercial ingredients were used: icing sugar (Tate & Lyle Sugars, London, UK), unsalted butter (Müller, Glasgow, UK), and native corn starch (Tesco Stores Ltd., Welwyn Garden City, UK). The composition of each ingredient supplied by the manufacturers was: icing sugar, 99.0% w/w carbohydrate; butter, 82.8% w/w fat and 1.0% w/w protein; and native corn starch, 88.0% w/w carbohydrate, 0.4% w/w protein, and 0.4% w/w fat.

Butter was softened at 30 °C using a heater before sample preparation. Icing sugar and native corn starch were sieved to remove particles larger than 75 μm using a 75 μm aperture British Test Sieve (Endecotts Ltd., London, UK). The native corn starch suspension (CSS, 50% w/w) was prepared by blending the starch with deionised water at room temperature (25 °C) using a magnetic stirrer (VMS-C4 Advanced, VWR International, UK) for 30 min.

Aerated icings were prepared in duplicate with the formulations given in Table 1. A traditional aerated icing recipe with a sugar: butter ratio of 2:1 was used as control (labelled Control). Partial butter replacement formulations labelled 25% BR and 50% BR were prepared with 25% and 50% of the butter by mass replaced with the CSS. The approximate volume fraction of each phase (φ_i) was calculated by (Rahman, 2009):

$$\varphi_i \approx \frac{w_i/\rho_i}{\sum_{j=1}^{m}(w_j/\rho_j)} \quad (1)$$

where w_i and ρ_i are the mass fraction [-] and density [kg m^{-3}] of phase i = [air, butter, CSS, sugar], respectively. The values calculated with Eq. (1) are subject to some uncertainty when the CSS is present as some of the sugar is expected to dissolve in the aqueous phase.

Ingredients were weighed to give a 450 g batch and whipped together at room temperature in a planetary mixer (Kenwood UK Ltd., Havant, UK) with a wire balloon-whisk agitator tool at speed setting 1 (approximately 60 rpm), giving a wall shear rate around 30 s^{-1} (Chesterton, Moggridge, Sadd, & Wilson, 2011). Two mixing times (t_m) were used (3 and 6 min) to give different air volume fractions (φ_{air}). The batch temperature was monitored before and after whipping using a thermometer, and no significant changes in temperature were observed. The whisked material was stored at 5 °C in sealed plastic containers for 16 h and left at room temperature for 1 h before analysis. Samples were considered to be stable during the experiments (no visible phase separation or change in macroscopic structure).

2.2. Air volume fraction

The φ_{air} was determined gravimetrically at room temperature using plastic dishes with known volume (25.5 cm^3). The dish was filled with icing and levelled off by a metal spatula. The filled dish was weighed and the density determined as the ratio of the formulation mass to the dish volume. Values of φ_{air} were calculated from (Torres et al., 2015a):

$$\varphi_{air} = 1 - \frac{\rho_A}{\rho_U} \quad (2)$$

where ρ_A and ρ_U are the densities of aerated and unaerated formulations [kg m^{-3}], respectively. All measurements were performed in triplicate.

2.3. Particle and bubble size distribution

The particle size distributions of sieved native corn starch and glazing sugar were determined using a Morphologi G3S automated optical particle characterisation system (Malvern Instruments Ltd., Malvern, UK). Additionally, the incorporation of the air phase was confirmed and evaluated using optical microscopy. The method was adapted from that reported by Chesterton et al. (2013) and Torres et al. (2015a). A small aliquot of sample was placed between two glass microscope slides, held 0.8 mm apart by plastic shims, and mounted in the Morphologi G3S microscope. Three photomicrographs were obtained for each formulation by capturing six preliminary microscopic fields at 10 × magnification and 80% intensity of bright field illumination. Image processing and analysis were performed using the open-source GNU Image Manipulation Program (GIMP 2.10.8) and image analysis conducted using the ImageJ 1.51w software tool (National Institute of Health, USA). An average of 210 bubbles were measured per photomicrograph.

The particle and bubble size distributions were fitted to a log-normal model:

$$f = \frac{1}{d\sqrt{2\pi\sigma^2}} e^{-\frac{[\ln(d)-x]^2}{2\sigma^2}} \quad (3)$$

where f is the normalised frequency [μm^{-1}], d is the particle or bubble

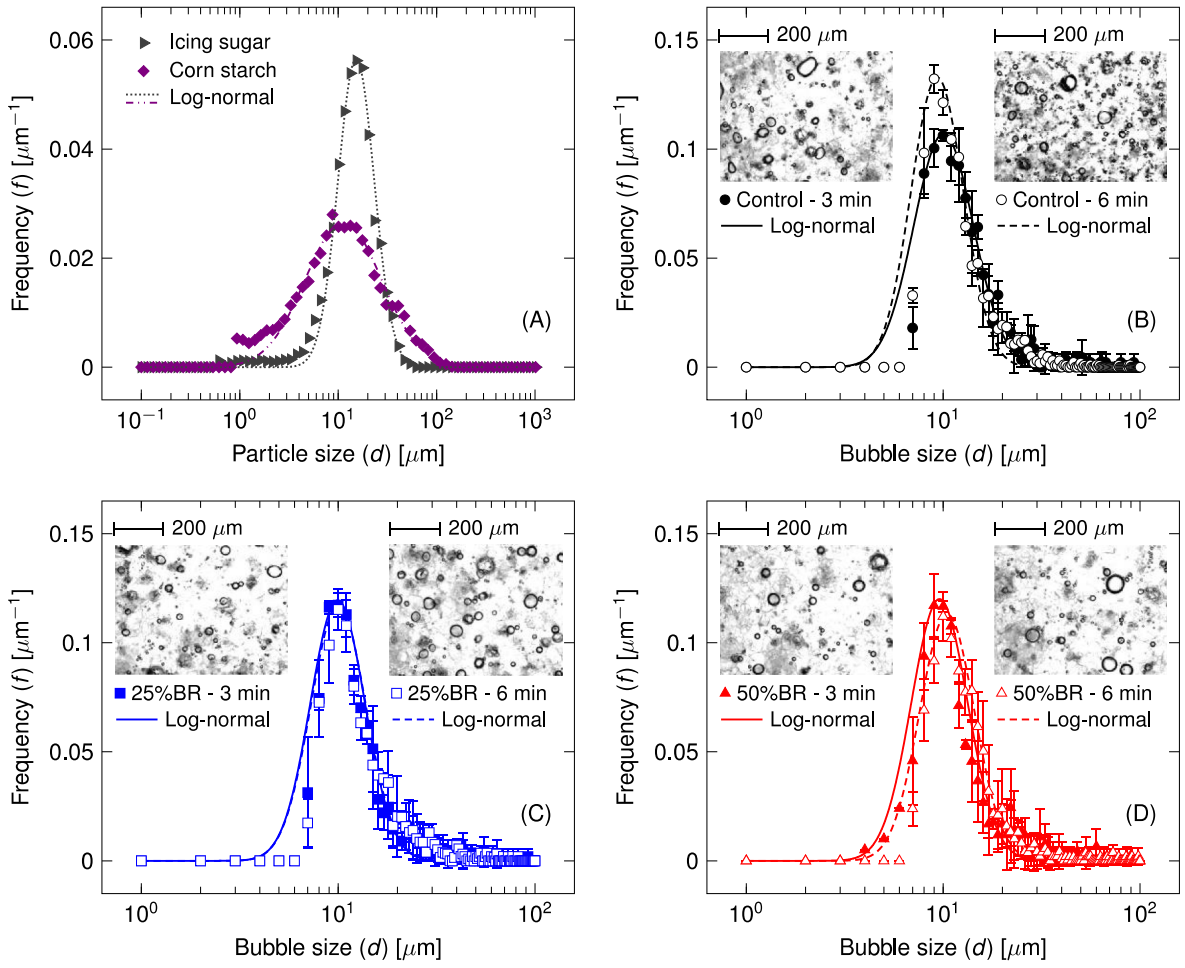

Fig. 1. (A) Particle size number (not volume) distributions of sieved commercial icing sugar and native corn starch used to make the aerated icings; (B-D) bubble size number (not volume) of aerated icings at different mixing times. Symbols are the mean size values of three replicates, error bars represent standard deviation and loci are the respective fitted log-normal distributions (Eq. (3)).

size diameter [μm], x is the mean of the distribution [-], and σ^2 is the variance of the distribution [-]. Here, $x = \ln(\bar{d})$ and $\bar{d}$ is the number mean size of the particles or bubbles [μm].

2.4. Rheological measurements and analysis

Rheological measurements were performed in duplicate using a controlled stress rheometer (Kinexus Lab+, Malvern Instruments Ltd., UK) equipped with 40 mm roughened parallel plates with 1.5 mm gap to reduce wall slip. Temperature was controlled at 25 °C using a water-cooled Peltier system. The sample was loaded on to the lower plate, taking care to prevent structural damage, and held at rest for 3 min before testing to allow temperature equilibration and material relaxation. After the gap was set, excess material was cleared away with a plastic spatula and the exposed edges were protected with a plastic cover to reduce water evaporation.

2.4.1. Stress sweeps

Stress sweeps ramps were performed by increasing the stress linearly from 1 to 200 Pa over 180 s (ramp rate 1.11 Pa s^{-1}). Plots of shear strain (γ) as a function of shear stress (τ) were inspected to give an estimate of the limit of elastic behaviour and the static yield stress (stress required to initiate flow) following the crossover line construction used by Meza, Peralta, and Zorrilla (2015; 2016).

2.4.2. Flow behaviour

Shear stress as a function of shear rate was determined in the range 0.2–3.2 s^{-1}, spanning the range expected for coatings draining under gravity (Lagarrigue & Alvarez, 2001). The data were fitted to the Bingham model for viscoplastic fluids (Steffe, 1996):

$$\tau = \tau_{0B} + \mu_{pl}\dot{\gamma} \quad (4)$$

where τ is the shear stress [Pa], $\dot{\gamma}$ is the shear rate [s^{-1}], τ_{0B} is the Bingham yield stress (related to the dynamic yield stress of the material obtained by extrapolation of a mathematical model at steady flow) [Pa], and μ_{pl} is the plastic viscosity [Pa s].

2.4.3. Creep and recovery tests

Creep tests, probing the behaviour of the icings after flow, were performed within the linear viscoelastic deformation regime at a fixed stress of 50 Pa. Preliminary experiments indicated that independency of the strain from the applied stress (compliance) started at 40 Pa. The stress was applied instantaneously, maintained for 180 s, and the strain determined as a function of time. After 180 s, the stress was removed and recovery measured over 180 s.

Creep and recovery behaviours were described using the solution (in the normalised form) of the four-component Burgers model (Supplementary Material) which features a Maxwell and a Kelvin-Voigt element in series (Findley, Lai, & Onaran, 1976; Ottosen & Ristinmaa, 2005):

$$\gamma^* = \frac{\tau_s}{\gamma_{max}} \left\{ \left(\frac{1}{G_0} + \frac{t_s}{\mu_0} t^* + \frac{1 - e^{-\frac{G_1 t_s}{\mu_1} t^*}}{G_1} \right) H(t^*) - \left[\frac{1}{G_0} + \frac{t_s}{\mu_0} (t^* - 1) + \frac{1 - e^{-\frac{G_1 t_s}{\mu_1} (t^* - 1)}}{G_1} \right] H(t^* - 1) \right\} \quad (5)$$

where γ^* is a normalised shear strain (γ/γ_{max}) [-], τ_s is the stress imposed in the step [Pa], t_s is the time when stress is removed [s], t^* is a dimensionless time defined as t/t_s [-], γ_{max} is the maximum shear strain (obtained at t_s) [-], and $H(y)$ is a Heaviside step function (1 if $y \geq 0$ and 0 if $y < 0$) [-]. The model has four fitted parameters: G_0 is the instantaneous elastic modulus of the Maxwell spring [Pa], G_1 is the elastic modulus of the Kelvin-Voigt spring [Pa], μ_0 is the Newtonian viscosity associated with the Maxwell dashpot [Pa s], and μ_1 is the internal viscosity associated with the Kelvin-Voigt dashpot [Pa s]. In the linear viscoelastic region, values of parameters obtained for the creep phase should be identical to those obtained for the recovery phase (Steffe, 1996). In the experiments, $t_s = 180$ s and $\tau_s = 50$ Pa.

The contribution of each elastic modulus to the maximum deformation to which the system is subjected can be expressed as:

$$\gamma_i^* = \frac{\tau_s / G_i}{\gamma_{max}} \quad (6)$$

where i = [0,1]. In addition, the level of recovery (R) of the system subjected to prior deformation can be determined from:

$$R = 1 - \frac{\gamma_\infty}{\gamma_{max}} \quad (7)$$

where γ_∞ is the shear strain at $t \to \infty$ [-] estimated by $\gamma_\infty = \tau_s t_s / \mu_0$ (Steffe, 1996).

2.5. Statistical analysis

Data were evaluated by analysis of variance (ANOVA) testing and Kruskal-Wallis ANOVA test was used when normality and homoscedasticity of samples were not obtained. When differences among samples and treatments were significant ($P < 0.05$), post hoc analyses were conducted. The parameters of Eqs. (4) and (5) were obtained by linear and non-linear regression, respectively. The goodness of fit of models was evaluated based on the mean absolute percentage error (*MAPE*):

$$MAPE = \frac{100}{n} \sum_{i=1}^{n} \left| \frac{x_{i,\,exp} - x_{i,\,theor}}{x_{exp}} \right| \quad (8)$$

where n is the number of samples, $x_{i,\,exp}$ is the i-th experimental value, and $x_{i,\,theor}$ is the i-th value predicted by the model. All statistical analyses were done using a Statgraphics Plus 5.1 software package (Statgraphics Inc., Rockville, MD, USA).

3. Results and discussion

3.1. Ingredient particle sizes

Fig. 1A shows that the icing sugar and native corn starch particle size distributions were roughly unimodal, with modal values of 11 and 15 μm, respectively. The maximum size for corn starch was observed at 120 μm, indicating some agglomeration, while the maximum icing sugar size was 60 μm. These data refer to the dry state; partial solubilisation of sugar in the aqueous parts of the continuous phases is expected. The native starch is partially crystalline and insoluble in water at room temperature (Biliaderis, 2009). The distributions for both ingredients were approximately log-normal and the fitted parameters were: $x_{sugar} = 3.223$, $\sigma^2_{sugar} = 0.8$, $x_{starch} = 2.902$, and $\sigma^2_{starch} = 0.18$.

3.2. Air volume fractions

The φ_{air} and ρ_A values for the aerated icings are reported in Table 2. The values increased with t_m, reaching 0.13–0.17 after 6 min, mirroring the trend reported for other aerated foods, such as whisked egg white and sugar (Lau & Dickinson, 2004) and bubbly liquids with carrageenan and guar gum solutions as the continuous phase (Torres et al., 2015a,b).

No significant differences were observed between the 25% BR and Control values of φ_{air} for a given t_m, indicating that this level of butter replacement did not affect the incorporation of air. The 50% BR formulation, however, gave consistently lower φ_{air} values than the Control. This effect was attributed to the increased shear viscosity of the samples arising from the shear-thickening introduced to the continuous phase by the high loading of the CSS (Section 3.4.2). Crawford et al. (2013) investigated the flow behaviour of native corn starch suspensions at 25 °C over a wide range of concentrations (10% w/w to 55% w/w) and found that samples exhibited shear-thickening behaviour at $\dot{\gamma}$ higher than 1 s^{-1}. The onset of thickening behaviour was observed at lower $\dot{\gamma}$, being more prominent as the corn starch concentration increased. The increase in viscosity was related to the formation of transient particle clusters generated when dispersed particles are forced into near contact with one another by strong shear stresses (Crawford et al., 2013). Steffe (1996) reported a flow curve for a 53% w/w CSS in which the apparent viscosity increased from 4 Pa s above $\dot{\gamma}$ of 5 s^{-1}. These effects are expected to arise at the mixer wall, where the highest local shear rates of approximately 30 s^{-1} are observed, leading to the entrapment of air bubbles.

3.3. Bubble sizes

Fig. 1B–D shows examples of images and bubble size distribution obtained for each formulation. Three materials gave approximately single-mode distributions, with modal values in the range of 8.4–10.7 μm, with maximum bubbles size values in the range of 80–100 μm. The distributions are approximately log-normal and values of x and σ^2 fitted for all samples are presented in Table 2. Mixing time and formulation did not affect the results. The bubble sizes are similar to those observed in

Table 2
Density (ρ_A), air volume fraction (φ_{air}), and the log-normal distribution parameters (x and σ^2) (Eq. (3)) of aerated icings at different mixing times (t_m). Mean values (± standard deviation) with different letters within a column are significantly different ($P < 0.05$).

Code	t_m [min]	ρ_A [kg m^{-3}]	φ_{air} [-]	x [-]	σ^2 [-]
Control	3	1148 ± 2	0.12 ± 0.02^b	2.430 ± 0.010^a	0.122 ± 0.003^a
	6	1083 ± 8	0.17 ± 0.01^c	2.328 ± 0.046^a	0.094 ± 0.008^a
25% BR	3	1214 ± 4	0.11 ± 0.00^b	2.398 ± 0.017^a	0.102 ± 0.004^a
	6	1145 ± 9	0.16 ± 0.01^c	2.408 ± 0.052^a	0.104 ± 0.026^a
50% BR	3	1264 ± 18	0.08 ± 0.01^a	2.368 ± 0.099^a	0.108 ± 0.019^a
	6	1197 ± 19	0.13 ± 0.01^b	2.451 ± 0.031^a	0.102 ± 0.023^a

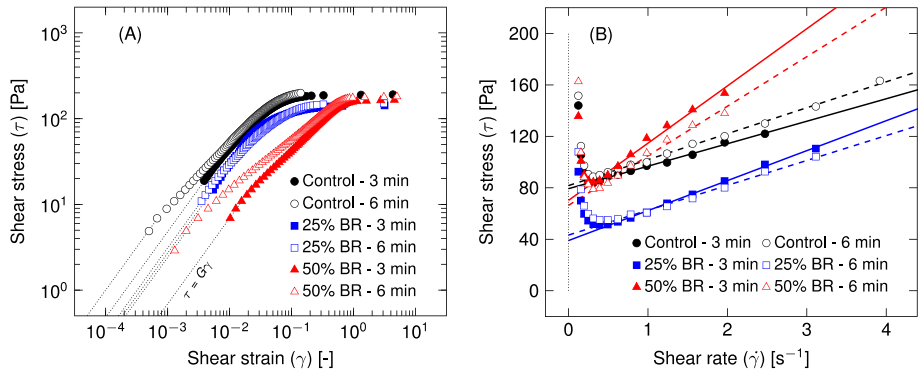

Fig. 2. (A) Representative strain-stress diagrams of aerated icings at different mixing times; (B) shear stress (τ) as a function of shear rate ($\dot{\gamma}$) for aerated icings at different mixing times. Symbols are one of two replicates. Loci represent Hookean elastic behaviour and the fit to the Bingham model (Eq. (4)).

Table 3
Values of elastic-limit yield stress (τ_{01}) and static yield stress (τ_{02}) for aerated icings at different mixing times (t_m) estimated from stress-strain curves (Fig. 4). Mean values (± standard deviation) with different letters within a column are significantly different ($P < 0.05$).

Code	t_m [min]	τ_{01} [Pa]	τ_{02} [Pa]
Control	3	37.3 ± 3.7^{d}	193 ± 3^{e}
	6	16.8 ± 0.6^{b}	–
25% BR	3	44.9 ± 1.3^{e}	139 ± 0^{a}
	6	24.4 ± 0.3^{c}	149 ± 3^{b}
50% BR	3	13.7 ± 1.0^{a}	167 ± 7^{c}
	6	11.8 ± 1.1^{a}	181 ± 7^{d}

aerated high sugar-egg albumen mixtures using confocal microscopy, where mean bubble sizes between 5 and 15 μm were obtained after 10 min of whisking (Lau & Dickinson, 2004).

Fig. 1 indicates that the mesoscale structural components of the aerated icing (sugar particles, starch granules, and bubbles) had similar sizes. The modal values are all significantly smaller than the 1.5 mm gap employed in the rheological tests, allowing bulk behaviour to be assessed. Bubble sizes can be used to estimate the capillary number (Ca):

$$Ca = \frac{\text{viscous forces}}{\text{capillary forces}} = \frac{\tau d}{2\sigma} \tag{9}$$

where σ is the air-fluid surface tension [mN m^{-1}]. Determination of σ for the butter-sugar matrix is complicated due to the effects of elasticity, but Ca can be estimated using the value of σ for 38% cream at 25 °C of 31 mN m^{-1} (Kristensen, Jensen, Madsen, & Birdi, 1997) as $Ca \approx 1.67 \times 10^{-4}\tau$. The bubbles (and also CSS droplets) are not expected to undergo significant deformation until Ca reaches a critical value. Chesterton et al. (2013) reported changes in flow behaviour in cake batters at Ca values greater than 0.02, corresponding here to $\tau \approx 120$ Pa.

Table 4
Parameters of the Bingham model (τ_{0B} and μ_{pl}) (Eq. (4)) for flow curves of aerated icings at different mixing times (t_m) (Fig. 5). Mean values (± standard deviation) with different letters within a column are significantly different ($P < 0.05$).

Code	t_m [min]	τ_{0B} [Pa]	μ_{pl} [Pa s]	*MAPE* [%]
Control	3	76.8 ± 3.6^{c}	19.9 ± 3.4^{ab}	1.11
	6	77.6 ± 5.8^{c}	22.2 ± 2.9^{ab}	1.13
25% BR	3	41.2 ± 3.1^{a}	23.1 ± 0.2^{b}	1.26
	6	52.5 ± 13.2^{ab}	17.1 ± 3.2^{a}	2.16
50% BR	3	76.9 ± 9.5^{c}	46.0 ± 2.2^{c}	1.77
	6	67.6 ± 1.7^{bc}	44.0 ± 7.7^{c}	1.49

3.4. Rheological behaviour

3.4.1. Stress sweeps

Stress sweeps for aerated icings are shown in Fig. 2A. They were performed to evaluate the static yielding behaviour, which might involve creep (Lidon, Villa, & Manneville, 2017) and plasticity (Donley, de Bruyn, McKinley, & Rogers, 2019; Fernandes, Andrade, Franco, & Negrão, 2017). Two changes in the slope of curves are evident. The first change corresponds to the elastic-limit yield stress (τ_{01}), *i.e.* the end of the elastic region and the start of creep (Chang, Boger, & Nguyen, 1998). The second change corresponds to the static yield stress (τ_{02}), which is attributed to the onset for flow (transition between solid and fluid behaviour) (Fernandes et al., 2017; Nguyen & Boger, 1992). The second change is characterised by a sudden increase of the strain and fracture or structural breakdown of the sample (Chang et al., 1998). The intermediate zone is characterised by creep.

Table 3 summarises the values of both elastic-limit and static yield stress. The τ_{01} values are similar in magnitude, ranging from 11.8 to 44.9 Pa, decreasing as t_m increases in Control and 25% BR samples. A similar trend was observed for the 50% BR sample, although this effect was not statistically significant. Fig. 2A suggests that inclusion of air bubbles in the three formulations increases the elastic modulus of the materials. Therefore, air inclusions promote brittle behaviour, which is probably a result of the local stress concentration around the bubbles. Additionally, replacing butter by the CSS leads to a decrease in τ_{02} indicating that the viscous CSS indeed acts as a plasticiser.

The values of τ_{02} are 5–7 times larger than τ_{01} and vary with the formulation. The value for Control at 3 min of aeration (193 Pa) gives $Ca \approx 0.03$, which is close to the critical number reported in Section 3.3. The Control formulation with 6 min of t_m did not exhibit yielding in the studied stress range, which is consistent with the increase in τ_{02} with t_m (and φ_{air}) observed for the two reduced-fat formulations, indicating that the limit for the flow behaviour is affected by the incorporation of air. These results are consistent with the low Ca regime: bubbles remain nearly spherical and exert an elastic response which is larger than that of the equivalent volume of the continuous phase. Ducloué, Pitois, Goyon, Chateau, and Ovarlez (2015) studied the rheological behaviour of dispersions of bubbles in model yield stress fluids and found that bubbles were stiff compared to the suspending emulsion at the point where yielding was observed.

The values of τ_{02} obtained for the reduced-fat formulations were lower than the Control samples prepared with the same t_m. The reduction for the 25% BR (which exhibit similar values of φ_{air}) can be attributed to the replacement of the continuous phase by the CSS, which has negligible bulk elasticity compared to butter.

The 50% BR data exhibit behaviour associated with an elastic modulus ($G = \tau/\gamma$) of ~700 Pa (Fig. 2A), where the Control and 25% BR values initially behave as a material with $G \approx 2 - 10$ kPa. These results indicate that there is a level of butter replacement at which the aerated

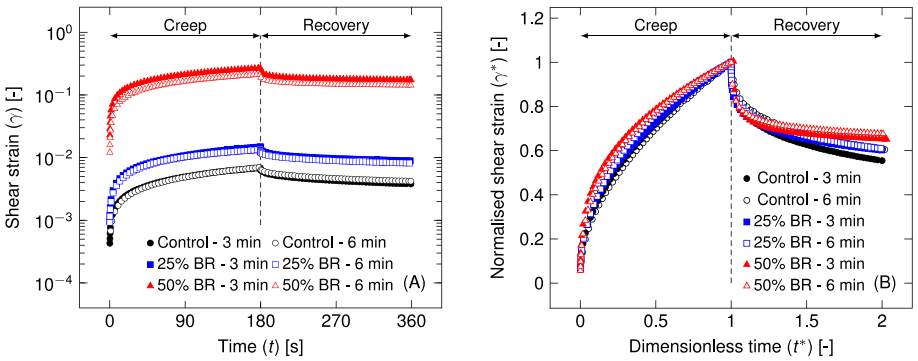

Fig. 3. Representative creep and recovery curves of aerated icings at different mixing times: (A) curves of strain (γ) as a function of time (t) and (B) curves of normalised shear strain (γ^*) as a function of dimensionless time (t^*). Symbols are one of two replicates.

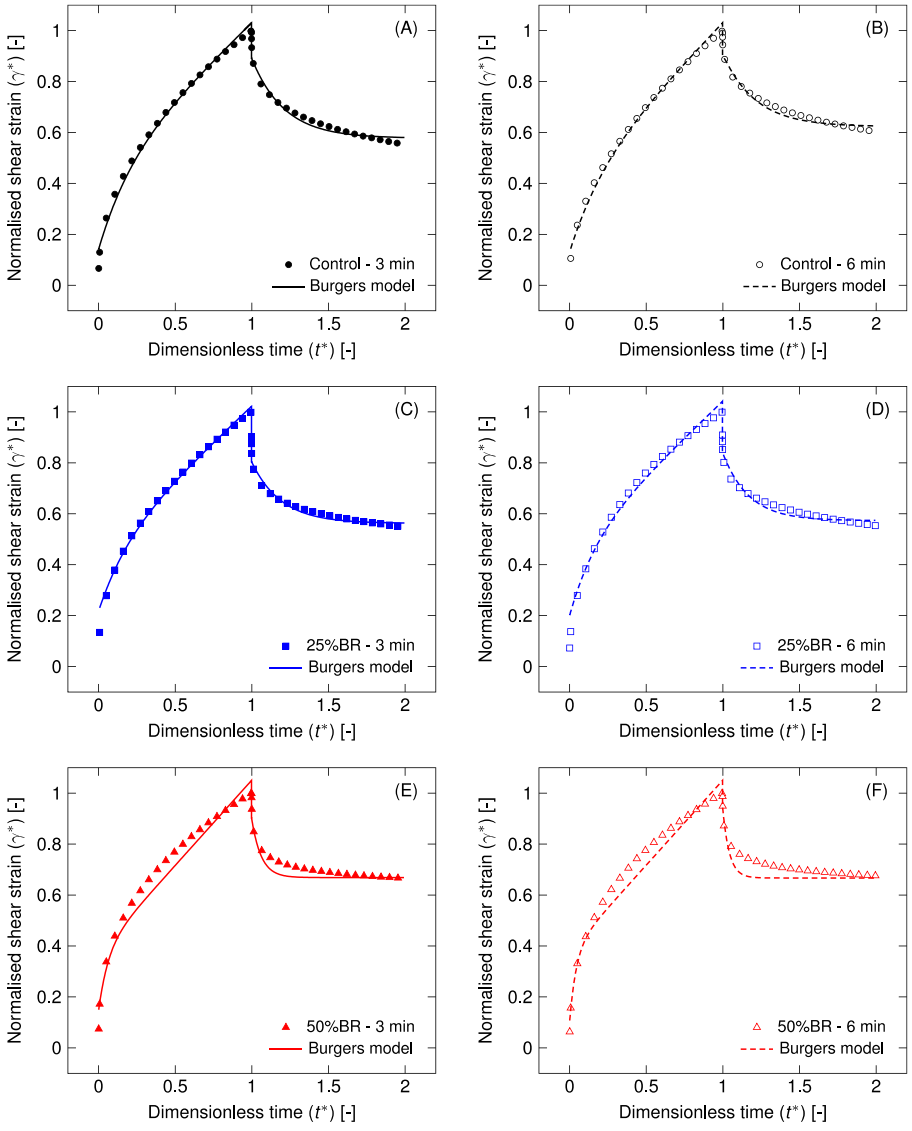

Fig. 4. Fit of the Burgers model (Eq. (5)) (loci) to creep and recovery experimental data for aerated icings at different mixing times. Symbols are experimental values of one of two replicates.

Table 5
Parameters of the Burgers model (G_0, G_1, μ_0, and μ_1) (Eq. (7)) obtained from creep-recovery testing of aerated icings at different mixing times (t_m) (Fig. 4). Mean values (± standard deviation) with different letters within a column are significantly different ($P < 0.05$).

Code	t_m [min]	G_0 ($\times 10^4$) [Pa]	G_1 ($\times 10^4$) [Pa]	μ_0 ($\times 10^4$) [Pa s]	μ_1 ($\times 10^4$) [Pa s]	*MAPE* [%]
Control	3	5.26 ± 0.14^{d}	2.87 ± 0.79^{c}	225 ± 2^{e}	89.0 ± 1.0^{c}	5.08
	6	6.03 ± 0.75^{d}	2.69 ± 0.17^{c}	207 ± 1^{d}	94.1 ± 6.4^{c}	3.82
25% BR	3	1.82 ± 0.37^{c}	1.32 ± 0.10^{b}	99.5 ± 11.9^{c}	37.2 ± 15.6^{b}	4.07
	6	1.92 ± 0.08^{c}	1.43 ± 0.06^{b}	112 ± 7^{c}	43.4 ± 1.0^{b}	4.75
50% BR	3	0.12 ± 0.00^{a}	0.08 ± 0.00^{a}	5.07 ± 0.14^{a}	0.81 ± 0.09^{a}	5.64
	6	0.29 ± 0.08^{b}	0.09 ± 0.01^{a}	6.35 ± 0.03^{b}	0.53 ± 0.18^{a}	5.75

icing will be noticeably different from the traditional recipe.

3.4.2. Steady flow

The shear strain ramps allow the behaviour in pumping and dispensing operations to be quantified. The rheograms in Fig. 2B exhibit viscoplastic behaviour, with steady flow occurring above a critical shear stress. The inclusion of air and butter replacement did not change the underlying flow behaviour.

At very low $\dot{\gamma}$ from 0.2 to 0.5 s^{-1}, τ decreased as $\dot{\gamma}$ increased, showing a negative slope in the $\tau - \dot{\gamma}$ plot. Cheng (1986) postulated that this observation could be due to the static yield stress. The range of $\dot{\gamma}$ was limited to 3.2 s^{-1} by experimental artefacts at higher τ associated with plastic behaviour and fracture above the yield point. Similar features were observed in aerated food systems (Lau & Dickinson, 2004).

The parameters obtained for the Bingham model (Eq. (4)) are presented in Table 4. The low errors (*MAPE* < 2.16%) indicate a good capacity of the model to describe the flow behaviour of all the aerated icings.

Inclusion of air did not affect the values of τ_{0B} for each formulation significantly. Values are consistently smaller than static yield stress values, with $\tau_{0B} \approx \tau_{02}/2.7$ (Tables 3 and 4), which might suggest a time-dependent yield stress behaviour (Møller, Fall, Chikkadi, Derks, & Bonn, 2009).

The difference in plastic viscosity μ_{pl} with φ_{air} was not significant for Control and 50% BR samples, whereas the decrease in μ_{pl} with the increase in φ_{air} for the 25% of butter replacement formulation was statistically significant. The impact of butter replacement is not simple. Adding starch at the 25% BR level reduced μ_{pl} around 25% and gave a small change in τ_{0B} after 6 min aeration (when the φ_{air} values were similar). Increasing the CSS level to 50% gave similar τ_{0B} values to the Control and μ_{pl} values approximately twice as large (Supplementary Material). This behaviour could be useful in a food coating process, where energy is supplied to induce flow of the film-forming material. In this case, a lower value of τ_{0B}, maintaining μ_{pl} and φ_{air} constant for the reduced-fat aerated icing, might be a beneficial aspect in comparison with the traditional version.

3.5. Creep and recovery behaviour

Raw and normalised creep and recovery data are presented in Fig. 3. The shape of the curves suggests that all the aerated icings behaved as viscoelastic solids. The creep phase can be characterised by an initial elastic deformation (spring of the Maxwell element) followed by a second and slower exponential-type deformation (Kelvin-Voigt element) tending towards an asymptote (and maximum strain) as $t_s \rightarrow \infty$ (corresponding to the dashpot of the Maxwell element). Thereafter, the recovery phase is characterised by a residual and irreversible deformation, which is characteristic of plasticity (Steffe, 1996). Full recovery was not observed, even 180 s after the τ_s was removed.

The fit to the Burgers model (Eq. (5)) is shown in Fig. 4 and the obtained parameters are presented in Table 5. The errors (*MAPE* < 5.75%) indicated that the model gave a good description of the creep and recovery behaviour. This result evidenced that, although aerated icings have shown elastoviscoplastic behaviour, they can be treated as simple viscoelastic materials and modelled with the Burgers model if evaluated below the yield limit. Another mechanical model (Kelvin-Voigt and Jeffreys) was also tested (Supplementary Material). However, the Burgers model has shown a better description of the data within both creep and recovery phases, due to the presence of G_0 necessary to describe the initial shear strain jump.

Table 5 shows that t_m did not influence the creep and recovery behaviour of all the samples, unlike the stress sweeps (Section 3.4.2) and steady shear (Section 3.4.1) tests. Some parameters evidenced a significant difference with t_m, such as G_0 and μ_0 for the 50% BR sample and μ_0 and μ_1 for the control sample. However, statistically significant differences were not observed for all the other parameters. The small bubble sizes may explain this behaviour, as their diameter is of the same order of the dimensions of the dispersed solid (Section 3.1). Creeping deformations in dispersed systems depend, for example, on the mechanical properties of the continuous phase, on the particle size distribution of the dispersed phase, on the type of stabilising agent, and on temperature (Pycia, Gałkowska, & Juszczak, 2017). Small bubbles in a viscoplastic media could behave as fillers, where their relative contribution to the elastic and viscous components to the overall rheology will depend on the applied rate of strain (Bee, Clement, & Prins, 2008; Ducloué et al., 2015). So, the viscous component allows the stress to relax over a certain low time scale (such as in creep tests performed in the linear viscoelastic regime), and a large or rapidly applied strain will produce a more elastic response (such as in stress sweeps). In the present work, the bubbles contribution to the linear viscoelastic behaviour of aerated icings was considered very small compared to that of the surrounding medium. This translates into negligible elastic contribution and viscous dissipation compared to the yield stress continuous phase fluid (Ducloué et al., 2015).

The Burgers model parameters were affected by the butter replacement (Table 5). The 25% BR and 50% BR samples showed lower μ_0 and G_0 (both related to the Maxwell element) than Control. The μ_0 characterises the linear region of the viscous shear strain because it measures the mechanical behaviour of the fluid part of the system (Dolz, Hernández, & Delegido, 2008; Steffe, 1996). Values of μ_0 are associated with the fluid behaviour of the continuous phase. The decrease in μ_0 may be related to the increase in the content of water-based continuous phase in reduced-fat formulations acting as a plasticiser and dissolving part of the sugar particles. In addition, the G_0 may be related to the undisturbed network structure of the samples. A lower value of G_0 may suggest a higher degree of non-retarded elastic-like deformation, indicating that the strands in the network structure are relatively free to rearrange between cross-links. The decrease in G_0 values with butter replacement indicates that the aerated icings become less rigid than Control full-fat counterpart, which is consistent with the decrease in stiffness observed with the increase in CSS content in the stress ramps.

Significant differences were observed in parameters related to the Kelvin-Voigt element (G_1 and μ_1), where both values decreased in reduced-fat formulations compared to Control (Table 5). Values of G_1 are the main component of the viscoelastic behaviour during creep, and

Table 6
Maximum shear strain (γ_{max}), percentage of participation on the shear strain of each elastic element of the Burgers model (γ_0^* and γ_1^*) (Eq. (8)), and the level of recovery (R) (Eq. (9)) for aerated icings at different mixing times (t_m). Mean values (± standard deviation) with different letters within a column are significantly different ($P < 0.05$).

Code	t_m [min]	γ_{max} ($\times 10^2$) [-]	γ_0^* ($\times 10^2$) [-]	γ_1^* ($\times 10^2$) [-]	R ($\times 10^2$) [-]
Control	3	0.65 ± 0.05^{a}	14.7 ± 0.8^{bc}	27.7 ± 5.3^{ab}	38.1 ± 5.7^{c}
	6	0.68 ± 0.03^{a}	12.3 ± 1.1^{b}	27.5 ± 0.7^{b}	36.1 ± 2.1^{bc}
25% BR	3	1.51 ± 0.05^{c}	18.7 ± 4.4^{d}	25.0 ± 1.0^{a}	39.9 ± 5.3^{bc}
	6	1.35 ± 0.01^{b}	19.3 ± 1.0^{d}	25.9 ± 1.3^{ab}	40.5 ± 2.9^{c}
50% BR	3	26.9 ± 0.1^{e}	15.0 ± 0.6^{c}	24.1 ± 0.8^{a}	34.0 ± 1.4^{ab}
	6	20.3 ± 1.1^{d}	8.83 ± 2.00^{a}	26.6 ± 2.1^{ab}	30.2 ± 4.1^{a}

it was related to the disruption and conversion of the bonds in the sample network (Pycia et al., 2017). A lower value of G_1 is associated with less rigid behaviour. In the same way, this behaviour is probably due to the presence of a higher content of water-based continuous phase acting as plasticiser or dissolving part of the dispersed particles.

A useful quantity that can be incorporated to the analysis is the retardation time (λ) of the Kelvin-Voight element, that is represented by $\lambda = \mu_1/G_1$ (Olivares, Zorrilla, & Rubiolo, 2009; Steffe, 1996). The estimation of λ values calculated with parameters presented in Table 5 are the following: 31 s, 35 s, 28 s, 30 s, 10 s, and 6 s for Control, 25% BR, and 50% BR with 3 and 6 min of mixing time, respectively. These values indicate a decreasing trend in λ as the butter replacement increase, more noticeable in samples 50% BR. The amount of λ is related to the time to achieve maximum deformation in a viscoelastic material. This also implies that λ is inversely related to network structure elasticity, because materials with large λ reach full deformation slowly. As discussed before, the effect of the CSS content could have a relevant effect in 25% BR samples by increasing their structural rigidity and λ. However, 50% BR samples had the opposite effect, because the plasticising and dissolving effect of the large water-based continuous phase content decreased λ, reducing the network interactions and its rigidity during creep.

Values of γ_{max} and percentage of participation on the shear strain of each elastic element are shown in Table 6. γ_{max} increased with the butter replacement and decreased with t_m in samples 25% and 50% BR. This tendency is also observed in Fig. 3A and is consistent with the results obtained for stress sweeps (Section 3.4.1). Values of γ_1^* did not present significant differences among samples, but γ_0^* was significantly affected by butter replacement. In general, the contribution of γ_1^* to the total deformation was greater than the contribution of γ_0^*, further suggesting that aerated icings display a viscoelastic behaviour rather than a purely elastic one.

The level of recovery at different t_m are shown in Table 6. The aerated icings with the larger reduced-fat content recovered up to approximately 30% of its maximum deformation, being 10% lower than full-fat ones. Also, formulations 25% BR evidenced the same R as Control. This tendency is also observed in Fig. 3B. This parameter provided further evidence that the elasticity of these aerated icings is determined by the composition of the formulation rather than φ_{air}.

Fig. 5 shows the effect of formulation on the Burgers model parameters. Increasing φ_{air} and φ_{butter} tended to increase the viscoelasticity of

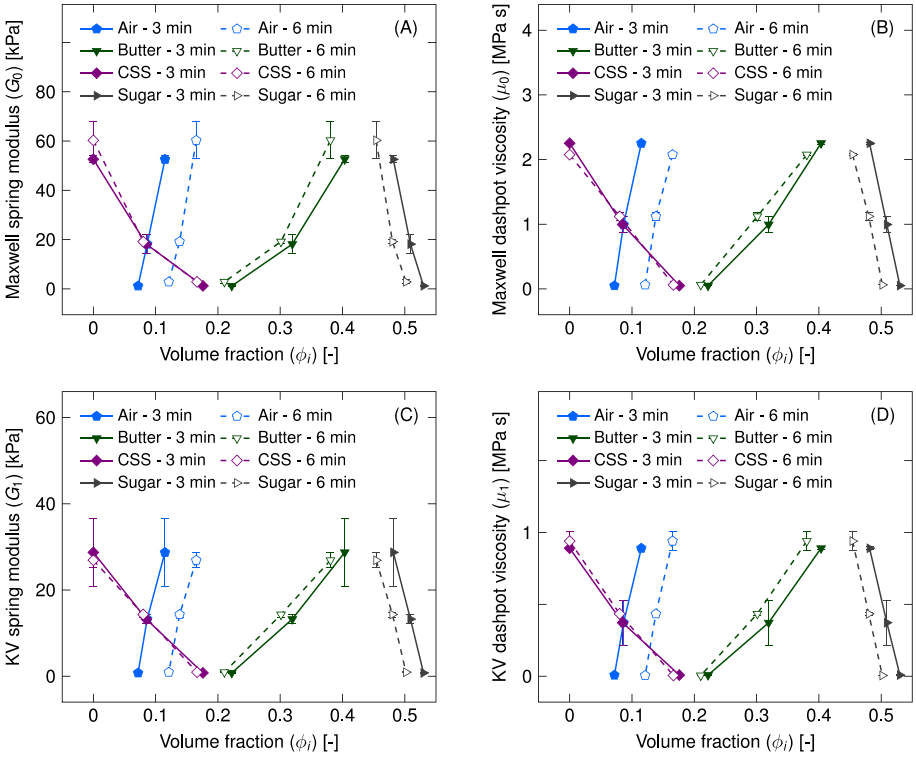

Fig. 5. Effect of formulation (estimated volume fraction of air, butter, CSS, and sugar) on Burgers parameters. (A) Maxwell spring modulus, (B) Maxwell dashpot viscosity, (C) Kelvin-Voigt (KV) spring modulus, and (D) Kelvin-Voigt (KV) dashpot viscosity. Solid lines – 3 min aeration; dashed lines - 6 min aeration.

the material, because the Burgers parameters increased. The butter is viscoplastic (Right et al., 2001; Vélez-Ruiz et al., 1997) and the air bubbles behave like rigid inclusions (Section 3.4.1). In addition, due to the larger number of rigid bubbles being present at higher φ_{air}, μ_0 and μ_1 increase. In addition, increasing the φ_{CSS} and φ_{sugar} tended to decrease the viscoelasticity of the icings, as indicated by the Burgers parameters decreasing. The CSS behaves as a viscous phase at the low $\dot{\gamma}$ involved in these tests, so an increase in its volume fraction reduces the rigidity of the material. At low γ, the apparent viscosity of a CSS is expected to be much smaller than that of the icings studied in this work (Steffe, 1996). For this reason, increasing the φ_{CSS} will reduce the overall viscosity, and hence μ_0 and μ_1. A decrease in the butter content results in a slight change in φ_{sugar}. It is expected that some of the sugar will be dissolved in the aqueous CSS. For this reason, the effect of φ_{sugar} on the parameters could not be determined conclusively.

4. Conclusions

The generation of aerated icings with reduced fat content was demonstrated and the impact on the product rheology was characterised systematically. In general, φ_{air} increased with mixing time. Bubble size distributions exhibited log-normal behaviour, with modal values of 9–11 μm for all formulations tested. Butter replacement at the 50% level reduced the amount of air incorporated, which was attributed to the shear-thickening behaviour of the starch phase.

The effect of the butter replacement on the flow behaviour was neither evident nor straightforward to describe as both parameters of the Bingham model (τ_{0B} and μ_{pl}) behave differently when changing the formulation. Rotational testing indicated viscoplastic behaviour with significant creep at low shear stresses. Above the upper limit of the yielding region the data fitted the Bingham model reasonably well. Creep and recovery experiments suggested that below the values of τ_{02}, the formulations exhibited significant viscoelasticity which could be described by the Burgers model. The parameters values of this model were significantly reduced by increasing the replacement of fat and remained unaffected by the mixing time.

CRediT authorship contribution statement

Bárbara E. Meza: Writing - original draft, preparation, Conceptualization, Methodology, Software, Validation, Formal analysis, Data curation, Visualization. **Rubens R. Fernandes:** Investigation, Conceptualization, Validation, Writing - review & editing. **Susana E. Zorrilla:** Conceptualization, Methodology, Supervision, Writing - review & editing, Resources, Project administration, Funding acquisition. **D. Ian Wilson:** Resources, Conceptualization, Methodology, Supervision, Writing - review & editing, Visualization, Project administration, Funding acquisition. **Juan Manuel Peralta:** Resources, Conceptualization, Methodology, Supervision, Writing - review & editing, Visualization, Project administration, Funding acquisition.

Declaration of competing interest

The authors declare that they have no known competing financial interests or personal relationships that could have appeared to influence the work reported in this paper.

Acknowledgements

This research was supported by CONICET, Argentina [Project PIP 2015-11220150100185CO and International Cooperation Project 2017-24020170100004CO]; Royal Society, UK [International Exchange IEC \R2\170130]; Coordenação de Aperfeiçoamento de Pessoal de Nível 600 Superior (CAPES) through a PhD scholarship for RRF, Brazil [Finance Code 001]; UNL, Santa Fe, Argentina [Project CAI + D 2016 50420150100002 LI]; and Agencia I + D + i, Argentina [Project PICT 2015-365].

Appendix A. Supplementary data

Supplementary data to this article can be found online at https://doi.org/10.1016/j.lwt.2021.111014.

References

Bee, R. D., Clement, A., & Prins, A. (2008). Behaviour of an aerated food model. In E. Dickinson (Ed.), *Food emulsions and foams*. Cambridge: Woodhead Publishing Limited.

Biliaderis, C. G. (2009). Structural transitions and related physical properties of starch. In J. BeMiller, & R. Whistler (Eds.), *Starch: Chemistry and technology* (3rd ed.). Amsterdam: Academic Press.

Campbell, G. M., & Mougeot, E. (1999). Creation and characterisation of aerated food products. *Trends in Food Science & Technology, 10*, 283–296. https://doi.org/10.1016/S0924-2244(00)00008-X

Chang, C., Boger, D. V., & Nguyen, Q. D. (1998). The yielding of waxy crude oils. *Industrial & Engineering Chemistry Research, 37*(4), 1551–1559. https://doi.org/10.1021/ie970588r

Cheng, D. (1986). Yield stress: A time-dependent property and how to measure it. *Rheologica Acta, 25*, 542–554. https://doi.org/10.1007/BF01774406

Chesterton, A. K. S., Moggridge, G. D., Sadd, P. A., & Wilson, D. I. (2011). Modelling of shear rate distribution in two planetary mixtures for studying development of cake batter structure. *Journal of Food Engineering, 105*, 343–350. https://doi.org/10.1016/j.jfoodeng.2011.02.044

Chesterton, A. K. S., Pereira de Abreu, D. A., Moggridge, G. D., Sadd, P. A., & Wilson, D. I. (2013). Evolution of cake batter bubble structure and rheology during planetary mixing. *Food and Bioproducts Processing, 91*(3), 192–206. https://doi.org/10.1016/j.fbp.2012.09.005

Crawford, N. C., Popp, L. B., Johns, K. E., Caire, L. M., Peterson, B. N., & Liberatore, M. (2013). Shear thickening of corn starch suspensions: Does concentration matter? *Journal of Colloid and Interface Science, 396*, 83–89. https://doi.org/10.1016/j.jcis.2013.01.024

Dolz, M., Hernández, M. J., & Delegido, J. (2008). Creep and recovery experimental investigation of low oil content food emulsions. *Food Hydrocolloids, 22*, 421–427. https://doi.org/10.1016/j.foodhyd.2006.12.011

Donley, G. J., de Bruyn, J. R., McKinley, G. H., & Rogers, S. A. (2019). Time-resolved dynamics of the yielding transition in soft materials. *Journal of Non-newtonian Fluid Mechanics, 264*, 117–134. https://doi.org/10.1016/j.jnnfm.2018.10.003

Ducloué, L., Pitois, O., Goyon, J., Chateau, X., & Ovarlez, G. (2015). Rheological behaviour of suspensions of bubbles in yield stress fluids. *Journal of Non-newtonian Fluid Mechanics, 215*, 31–39. https://doi.org/10.1016/j.jnnfm.2014.10.003

Eley, R. R. (2005). Applied rheology in the protective and decorative coatings industry. *Rheology Reviews*, 173–240.

Fernandes, R. R., Andrade, D. E. V., Franco, A. T., & Negrão, C. O. R. (2017). The yielding and the linear-to-nonlinear viscoelastic transition of an elastoviscoplastic material. *Journal of Rheology, 61*(5), 893–903. https://doi.org/10.1122/1.4991803

Findley, W. N., Lai, J. S., & Onaran, K. (1976). *Creep and relaxation of nonlinear viscoelastic materials*. Amsterdam: North-Holland Publishing Company.

Glass, B. E., Murphy, M. C., & Santori, N. (1992). *Reduced fat ready-to-spread frosting. United States Patent #5102680*.

Gómez, M. (2008). Low-sugar fat sweet goods. In S. G. Sumnu, & S. Sahin (Eds.), *Food engineering aspects of baking sweet goods*. Boca Raton: CRC Press.

Kristensen, D., Jensen, P. Y., Madsen, F., & Birdi, K. S. (1997). Rheology and surface tension of selected processed dairy fluids: Influence of temperature. *Journal of Dairy Science, 80*(10), 2282–2290. https://doi.org/10.3168/jds.S0022-0302(97)76177-0

Lagarrigue, S., & Alvarez, G. (2001). The rheology of starch dispersions at high temperatures and high shear rates: A review. *Journal of Food Engineering, 50*(4), 189–202. https://doi.org/10.1016/S0260-8774(00)00239-9

Lau, K., & Dickinson, E. (2004). Structural and rheological properties of aerated high sugar systems containing egg albumen. *Journal of Food Science, 69*(5), E232–E239. https://doi.org/10.1111/j.1365-2621.2004.tb10714.x

Lidon, P., Villa, L., & Manneville, S. (2017). Power-law creep and residual stresses in a carbopol gel. *Rheologica Acta, 56*, 307–323. https://doi.org/10.1007/s00397-016-0961-4

Lobato-Calleros, C., Ramírez-Santiago, C., Vernon-Carter, E. J., & Alvarez-Ramirez, J. (2014). Impact of native and chemically modified starches addition as fat replacers in the viscoelasticity of low-fat stirred yogurt. *Journal of Food Engineering, 131*, 110–115. https://doi.org/10.1016/j.jfoodeng.2014.01.019

Lucca, P. A., & Tepper, B. J. (1994). Fat replacers and the functionality of fat in foods. *Trends in Food Science & Technology, 3*, 12–19. https://doi.org/10.1016/0924-2244(94)90043-4

McNeill, G. P. (2014). Processing solutions: Fractionation and blended oils. In D. R. Kodali (Ed.), *Trans fats replacement solutions*. Illinois: AOCS Press.

Meza, B. E., Peralta, J. M., & Zorrilla, S. E. (2015). Rheological properties of a commercial food glaze material and their effect on the film thickness obtained by dip coating. *Journal of Food Process Engineering, 38*(5), 510–516. https://doi.org/10.1111/jfpe.12181

Meza, B. E., Peralta, J. M., & Zorrilla, S. E. (2016). Rheological characterization of full-fat and low-fat glaze materials for foods. *Journal of Food Engineering, 171*, 57–66. https://doi.org/10.1016/j.jfoodeng.2015.10.012

Møller, P. C. F., Fall, A., Chikkadi, V., Derks, D., & Bonn, D. (2009). An attempt to categorize yield stress fluid behaviour. *Philosophical Transactions. Series A, Mathematical, Physical, and Engineering Sciences, 367*, 5139–5155. https://doi.org/10.1098/rsta.2009.0194, 1909.

Morehouse, A. L., & Lewis, C. J. (1985). *Low-fat spread. United states patent #4536408*.

Nguyen, Q. D., & Boger, D. V. (1992). Measuring the flow properties of yield stress fluids. *Annual Review of Fluid Mechanics, 24*, 47–88. https://doi.org/10.1146/annurev.fl.24.010192.000403

Olivares, M. L., Zorrilla, S. E., & Rubiolo, A. C. (2009). Rheological properties of mozzarella cheese determined by creep/recovery tests: Effect of sampling direction, test temperature and ripening time. *Journal of Texture Studies, 40*, 300–318. https://doi.org/10.1111/j.1745-4603.2009.00183.x

Ottosen, N. S., & Ristinmaa, M. (2005). *The mechanics of constitutive modelling*. Amsterdam: Elsevier B.V.

Pycia, K., Gałkowska, D., & Juszczak, L. (2017). Maltodextrins produced from chemically modified starches as agents affecting stability and rheological properties of albumin foam. *Lebensmittel-Wissenschaft und -Technologie- Food Science and Technology, 80*, 394–400. https://doi.org/10.1016/j.lwt.2017.03.002

Rahman, M. S. (2009). *Food properties handbook*. Boca Raton: CRC Press.

Right, A. J., Canlon, G. S., Hartel, R. W., & Marangoni, A. G. (2001). Rheological properties of milkfat and butter. *Journal of Food Science, 66*, 1056–1071. https://doi.org/10.1111/j.1365-2621.2001.tb16082.x

Rønholt, S., Mortensen, K., & Knudsen, J. C. (2013). The effective factors on the structure of butter and other milk fat-based products. *Comprehensive Reviews in Food Science and Food Safety, 12*, 468–482. https://doi.org/10.1111/1541-4337.12022

Serinyel, G., & Öztürk, S. (2016). Investigation on potential utilization of native and modified starches containing resistant starch as a fat replacer in bakery products. *Starch, 68*, 1–9. https://doi.org/10.1002/star.201600022

Shay, G. D. (1995). Thickeners and rheology modifiers. In J. V. Koleske (Ed.), *Paint and coating testing manual* (14th ed.). Philadelphia: ASTM.

Singh, J., Dartois, A., & Kaur, L. (2010). Starch digestibility in food matrix: A review. *Trends in Food Science & Technology, 21*, 168–180. https://doi.org/10.1016/j.tifs.2009.12.001

Steffe, J. F. (1996). *Rheological methods in food process engineering*. Michigan: Freeman Press.

Torres, M. D., Gadala-Maria, F., & Wilson, D. I. (2013). Comparison of the rheology of bubbly liquids prepared by whisking air into a viscous liquid (honey) and a shear-thinning liquid (guar gum solutions). *Journal of Food Engineering, 118*, 213–228. https://doi.org/10.1016/j.jfoodeng.2013.04.002

Torres, M. D., Hallmark, B., & Wilson, D. I. (2015a). Effect of bubble volume fraction on the shear and extensional rheology of bubbly liquids based on guar gum (a Giesekus fluid) as continuous phase. *Journal of Food Engineering, 146*, 129–142. https://doi.org/10.1016/j.jfoodeng.2014.09.012

Torres, M. D., Hallmark, B., & Wilson, D. I. (2015b). Determination of the shear and extensional rheology of bubbly liquids with a shear-thinning continuous phase. *Rheologica Acta, 54*(6), 461–478. https://doi.org/10.1007/s00397-014-0832-9

Vélez-Ruiz, J. F., Barbosa Cánovas, G. V., & Peleg, M. (1997). Rheological properties of selected dairy products. *Critical Reviews in Food Science and Nutrition, 37*, 311–359. https://doi.org/10.1080/10408399709527778

Wang, B., Wang, L., Li, D., Zhou, Y., & Özkan, N. (2011). Shear-thickening properties of waxy maize starch dispersions. *Journal of Food Engineering, 107*, 415–423. https://doi.org/10.1016/j.jfoodeng.2011.06.011

Zúñiga, R. N., & Aguilera, J. M. (2008). Aerated food gels: Fabrication and potential applications. *Trends in Food Science & Technology, 19*, 176–187. https://doi.org/10.1016/j.tifs.2007.11.012